ACCELERATOR PHYSICS AND TECHNOLOGY CHALLENGES OF VERY HIGH ENERGY HADRON COLLIDERS

VLADIMIR D. SHILTSEV

Fermi National Accelerator Laboratory
*Batavia, IL 60510, USA**
shiltsev@fnal.gov

Received (Day Month Year)
Accepted (Day Month Year)

High energy hadron colliders have been in the forefront of particle physics for more than three decades. At present, international particle physics community considers several options for a 100 TeV proton-proton collider as a possible post-LHC energy frontier facility. The method of colliding beams has not fully exhausted its potential but has slowed down considerably in its progress. This paper briefly reviews the accelerator physics and technology challenges of the future very high energy colliders and outlines the areas of required research and development towards their technical and financial feasibility.

Keywords: colliders; accelerators; Tevatron.

PACS numbers: 29.20.-c, 29.20.Ej, 29.27.-a, 41.75.Jv, 52.27.Lw, 52.38.Kd

1. Colliding Beams: Introduction

Particle accelerators have been widely used for physics research since the early 20th century and have greatly progressed both scientifically and technologically since then. To gain insight into the physics of elementary particles, one accelerates them to a very high kinetic energy, lets them impact on other particles and detect products of the reactions that transform the particles into other particles. It is estimated that in the post-1938 era, accelerator science has influenced almost 1/3 of physicists and physics studies and on average contributed to physics Nobel Prize-winning research every 2.9 years [1]. Colliding beam facilities which produce high-energy collisions (interactions) between particles of approximately oppositely directed beams did pave the way for progress since the 1960's.

The center of mass energy E_{cm} for a head-on collision of two particles with masses m_1, m_2 and energies E_1 and E_2 is

$$E_{cm} = \left[2E_1E_2 + (m_1^2 + m_2^2)c^4 + 2\sqrt{E_1^2 - m_1^2c^4}\sqrt{E_2^2 - m_2^2c^4}\right]^{1/2} . \qquad (1)$$

For many decades, the only arrangement for accelerator experiments was a fixed target setup where a beam of particles accelerated with a particle accelerator hit a stationary target

*Fermi Research Alliance, LLC operates Fermilab under contract no. DE-AC02-07CH11359 with the U.S. Department of Energy

Operated by Fermi Research Alliance, LLC under Contract No. De-AC02-07CH11359 with the United States Department of Energy.

set into the path of the beam. In this case, as follows from Eq. (1), for high energy accelerators $E >> mc^2$, the CM energy is $E_{cm} \approx (2Emc^2)^{1/2}$. For example, 50 TeV = 50,000 GeV protons hitting stationary protons can produce reactions with about 304 GeV energy. A more effective colliding beam set-up in which two beams of particles are accelerated and directed against each other, has a much higher center of mass energy of $E_{cm} \approx 2(E_1E_2)^{1/2}$. In the case of two equal mass of particles (e.g. protons and protons, or protons and antiprotons) colliding with the same energy E of 50,000 GeV, one gets $E_{cm}=2E$ or 100,000 GeV. Such an obvious advantage secured the place of the colliders as the frontier high energy physics machines starting in the 1960's [2, 3].

Almost three dozen colliders reached the operational stage between the late 50's and now. Schematic drawings of several collider types are shown in Fig.1. In storage ring configurations - Fig.1a and 1b – particles of each beam circulate and repeatedly collide. This can be done in a single ring if the beams consist of the same energy antiparticles. In linear colliders, first proposed in Ref. [4], the beams are accelerated in linear accelerators (linacs) and transported to a collision point either in the simple two linac configurations depicted in Fig.1c, or with use of the same linac and two arcs as in Fig.1.d. Another possible linac-ring configuration is shown in Fig.1e.

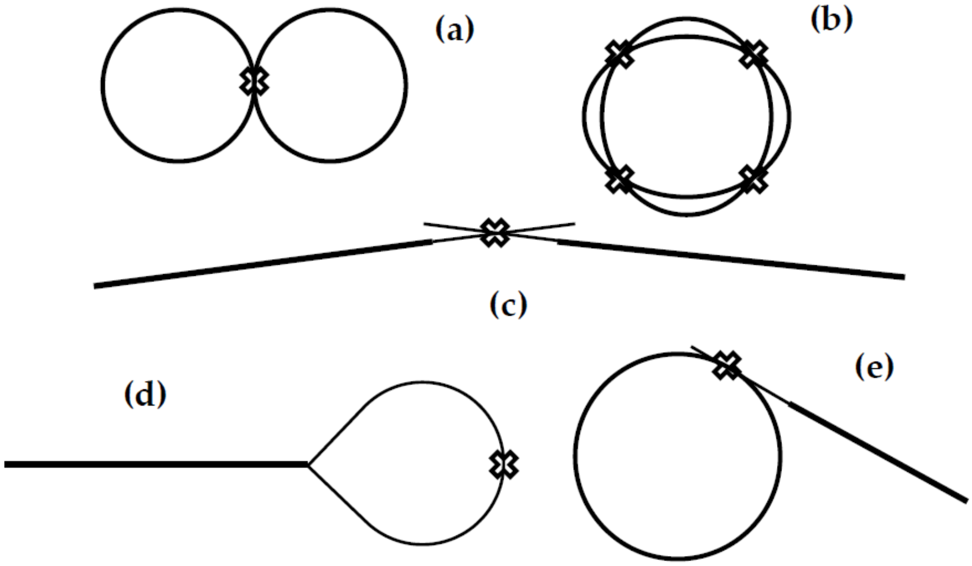

Figure 1: Schematics of particle collider types (from [3]).

The first lepton (*e-e-* or *e-e+*) colliders were built in the early 1960s almost simultaneously at three laboratories: AdA collider at the Frascati laboratory near Rome in Italy, the VEP-1 collider in the Novosibirsk Institute of Nuclear Physics (USSR) and the Princeton-Stanford Colliding Beam Experiment at Stanford (USA). In all three colliders their center of mass energies were 1 GeV or less. Construction of the first hadron (proton-proton) collider, the Intersecting Storage Rings, began at CERN (Switzerland) in 1966, and in 1971, this collider was operational and eventually reached E_{cm}=63 GeV. In the case of electrons and positrons the synchrotron radiation results in fast damping of betatron and synchrotron oscillations and creates an effective way to accumulate large currents. The synchrotron radiation has negligible effect on damping of particle oscillations in proton (hadron) colliders and therefore, a construction of proton-antiproton colliders required damping based on a mechanism another than the synchrotron radiation. The invention of the stochastic cooling technique in 1969 led to the construction of the first proton-antiproton collider $\mathrm{Sp\overline{p}S}$ at CERN in 1982. Many electron-positron and hadron collidershave been built over the past half-century – see, e.g. [2]. The Tevatron proton-antiproton collider [5] was the world's highest energy collider for almost 25 years since its operation began in December of 1985 until it was overtaken by the LHC in 2009 [6].

The energy of colliders has been increasing over the years as demonstrated in Fig.2. There, the triangles represent maximum CM energy and the start of operation for lepton colliders (usually, *e+e-*) and full circles are for hadron (protons, antiprotons, ions, proton-electron) colliders. One can see that until the early 1990's, the CM energy on average increased by a factor of 10 every decade and notably, the hadron colliders were 10-20 times more powerful. Since then, following the demands of high energy physics, the paths of the colliders diverged to reach record high energies in the particle reaction. The Large Hadron Collider (LHC) was built at CERN, while new *e+e-* colliders called "particle factories" were focused on detail exploration of phenomena at much lower energies.

Figure 2: Energy reach of particle colliders (adapted from [3]).

Hadron circular colliders employing superconducting high-field magnets – often called *supercolliders* - so far have dominated the energy frontier. The reason for this is the superconducting magnet technology offered the highest energy reach at an affordable cost. In the supercolliders, as in any circular accelerator, the maximum momentum and energy of ultra-relativistic particle is determined by the radius of the ring *R* and average magnetic field *B* of bending magnets:

$$pc = eB \cdot R \quad \text{or} \quad E[GeV] = 0.3 \cdot B[T] \cdot R[m]. \qquad (2)$$

Therefore, the energy evolution is driven by practical considerations: e.g., maximum field of normal conducting magnets of about 2T at some moment was not adequate for the energy demands because of required longer accelerator tunnels and increasing magnet power consumption. The development of superconducting (SC) magnets [7] – see Fig.3 - which employ high electric current carrying NbTi wires cooled by liquid Helium below 5K, opened the way to higher fields and record high energy hadron colliders. The latest of them, 14 TeV c.m. LHC at CERN uses 8.3T double bore magnets in 26.7 km circumference tunnel.

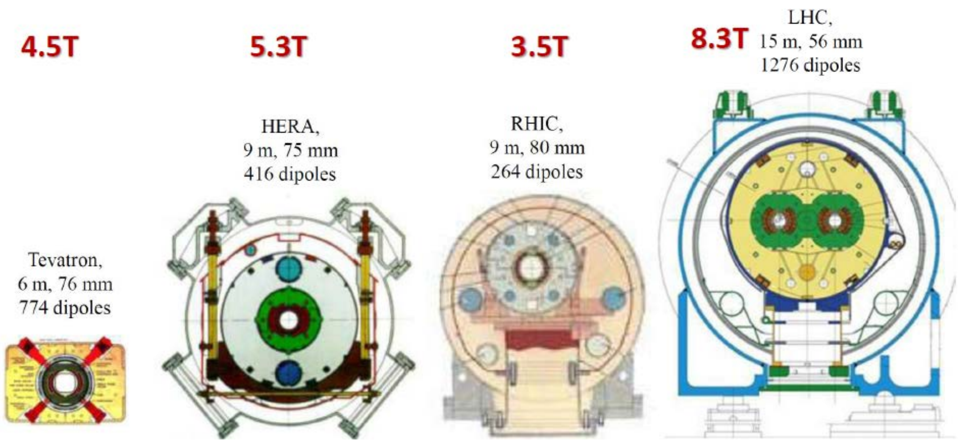

Figure 3: Superconducting dipole magnets for high energy hadron colliders: Tevatron (NbTi, warm-iron, small He plant, 4.5K), HERA (NbTi, Al collar, cold iron), RHIC (simple and economical design) and LHC (2K super fluid He, double bore) (from [3]).

To remain superconducting, such magnets need to operate within very strict limits on the power deposited into the low-temperature components (vacuum pipes, cold iron, SC cable, etc.) – typically on the order of 1 W/m or less, and that makes them of no practical use in high energy lepton accelerators, as relativistic electrons and positrons quickly lose energy due to the synchrotron radiation:

$$\delta E = \frac{4\pi}{3}\frac{e^2\gamma^4}{R} = 88.5[\frac{keV}{turn}]\cdot\frac{E^4[GeV]}{R[m]} \qquad (3).$$

The total power radiated into the walls reaches becomes prohibitively high, and, e.g., 22 MW or about 800 W/m even in the largest radius *e+e-* collider LEP (in the same tunnel, which is now occupied by LHC), at the beam energy of 105 GeV and relatively low average beam current of 4mA. Besides the need to replenish electron beam power by accelerating RF cavities, the synchrotron radiation leads to significant heating and outgassing of the beam vacuum pipe. On the other hand, the attainment of sufficiently long lifetimes of continuously circulating beams requires gas pressures of 1-10 nTorr or better. This technological challenge been successfully resolved in modern colliding "factories" operating with lower energy multi-Ampere beams. Radiation of protons (ions) is smaller by a significant factor $(\gamma_p/\gamma_e)^4=(m_e/m_p)^4$ – see Eq.(3) - but still can be of a certain concern at very high energy, high current SC accelerators, e.g., LHC.

Though only three hadron supercolliders reached operational stage; the Tevatron, the Relativistic Heavy Ion Collider (RHIC) [8], and LHC (see Fig.4) there were two notable examples of very large supercollider projects in the past, namely, the Superconducting SuperCollider in Texas, USA [9] and the UNK collider in Protvino, Russia [10]. Due to various reasons, mostly attributed to their scale, cost and complexity, they were terminated in 1991 and 1993, respectively [11]. Even larger *p-p* supercolliders were proposed – the Very Large Hadron Collider (VLHC) in the US in early 2000's [12], and more recently, the Future Circular Collider (FCC) at CERN and the Super Proton-Proton Collider (SppC) in China [13] – see Table 1.

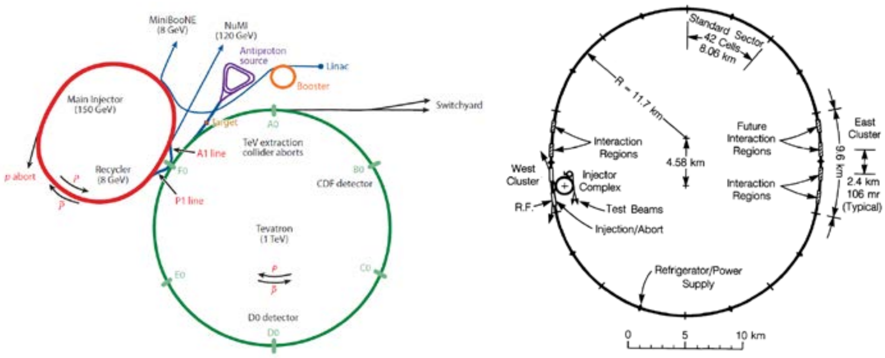

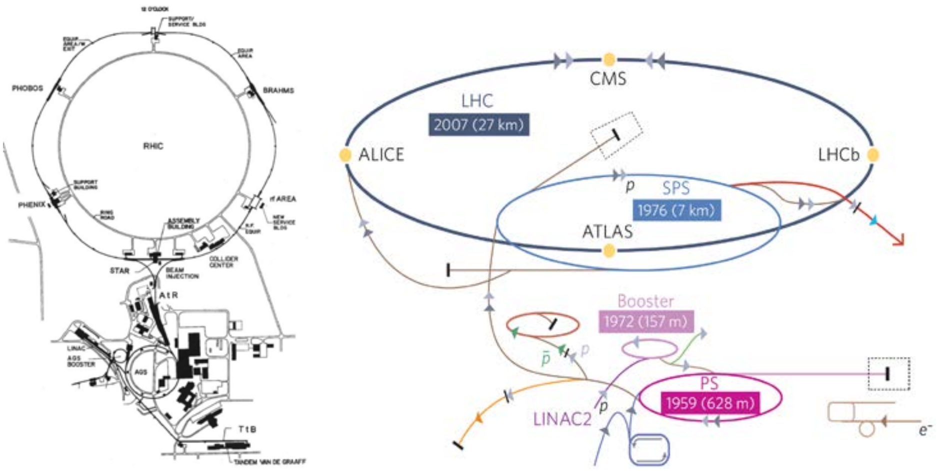

Fig. 4: Layouts of the superconducting hadron supercolliders (clockwise, from top left): the Tevatron (from Ref.[5]), SSC (from Ref.[9]), LHC (from Ref.[14]), and RHIC (from Ref.[8]).

Table 1: Hadron superconducting supercolliders and their construction costs (for the SSC, RHIC and LHC – see [15] and references therein, for the Tevatron and UNK – Refs. [16] and [17], correspondingly).

	Energy TeV, c.m.	Circumfe-rence, km	Cost (year)	Comments
Tevatron	1.96	6.3	0.45B$ (1986)	Operational, 1985-2011
SSC	40	87.1	11.8B$ (1993)	Terminated in 1993
UNK	6	20.8	~2B$ (1991)	Project stopped in 1998
RHIC	0.5	3.8	0.66B$ (2000)	Operational, 2000-present
LHC	14	26.7	6.5BCHF(2009)	Operational, 2008-present
FCC/SPPC	~100	~100	?	~2035 ?

Despite the fact that these accelerators were and are the largest and the most expensive instruments for high-energy physics research, they are quite cost-effective. For example, a comparative analysis [15] of publicly available costs for 17 large accelerators of the past, present and those currently in the planning stage has shown that the "total project cost (TPC)" (sometimes cited as "the US accounting") of a collider can be broken up into three major parts corresponding to "civil construction", "accelerator components", "site power infrastructure" and the three corresponding cost components can be parameterized by just three parameters – the length of the accelerator tunnel L, the center-of-mass or beam energy E, and the total required site power P. It was found that over almost 3 orders of magnitude of L, 4.5 orders of magnitude of E and more than 2 orders of magnitude of P the "$\alpha\beta\gamma$-cost model" works with ~30% accuracy:

$$Total\ Project\ Cost \approx \alpha \times Length^{1/2} + \beta \times Energy^{1/2} + \gamma \times Power^{1/2} \quad , \qquad (4)$$

where coefficients $\alpha = 2B\$/(10\ km)^{1/2}$, $\gamma = 2B\$/(100MW)^{1/2}$, and accelerator technology dependent coefficient β is equal to $10\ B\$/TeV^{1/2}$ for superconducting RF accelerators, $8\ B\$/\ TeV^{1/2}$ for normal-conducting ("warm") RF, $1B\$/TeV^{1/2}$ for normal-conducting magnets and $2B\$/TeV^{1/2}$ for SC magnets (all numbers in 2014 US dollars) – see Fig.5. Given that SC magnets provide a factor of ~5 higher magnetic fields (and correspondingly shorter tunnels) they allow for the reduction of the facility power by ~order of magnitude;it is not surprising to see that the supercolliders offer the highest energy reach within limited financial resources. Still, very high total costs of the supercolliders usually call for maximum possible performance (luminosity, see next section), various measures to reduce the cost (extensive R&D on the cost-effective magnets [18] and tunneling, re-use of the existing infrastructure and accelerator as injectors, etc.) and often the expansion of the physics program beyond *p-p* collisions (e.g., RHIC and LHC collider ions as well as protons).

Fig. 5: Estimated cost of the SC magnets and associated elements vs collider center of mass energy or single beam energy. Stage I of the VLHC assumed low-field 2T superferric magnets (from [15]).

2. Luminosity and Beam Dynamics Issues in Very High Energy Hadron Colliders

The exploration of rare particle physics phenomena requires appropriately high energy but also a sufficiently large number of detectable reactions. In a collider, the number of the events of interest per second depends on the cross section σ_{event} of the reaction under study is given by:

$$dN_{event} / dt = L \cdot \sigma_{event} \quad , \qquad (5)$$

where L is the collider luminosity. The luminosity depends only on the beam parameters and for a Gaussian beam distribution is:

$$L = \gamma f_0 \frac{N_B N_{p,1} N_{p.2}}{4\pi\beta^* \varepsilon} F(\sigma_s, \beta^*, \theta) \quad , \qquad (6)$$

where $N_{p(1,2)}$ is the number of particles per bunch in each of the two colliding beams, N_B is the number of bunches per beam, ε is the average rms normalized emittances of two round beams $(\varepsilon_{p1}+\varepsilon_{p2})/2$, $F<1$ is the geometric luminosity reduction factor, γ is the relativistic factor, and f_0 is the revolution frequency. Usually, for proton-proton colliders bunch intensities and emittances are about the same $N_{p1}=N_{p2}=N_p$ and $\varepsilon_{p1}=\varepsilon_{p2}=\varepsilon_p$, while that is not true for beams of different species, e.g., in the Tevatron proton-antiproton collider $N_p>>N_a$ and $\varepsilon_p>>\varepsilon_a$. The geometric luminosity reduction factor F takes into account the "hourglass effect" (variation of the transverse beam size along the luminous region) which depends on the ratio of the rms bunch length σ_s and beta-function at the collision point β^* and/or reduction due to crossing angle θ between two beam orbits at the interaction point (IP). For example, for round beams with $\sigma_s<<\beta^*$ and equal rms beam sizes σ^* at the IP for both beams:

$$F = \frac{1}{\sqrt{1+\left(\frac{\theta\sigma_s}{2\sigma^*}\right)}} \quad . \qquad (7)$$

Therefore, to achieve high luminosity, one has to maximize population of bunches with as low as possible emittances and to collide them at high frequency at the locations where the focusing beam optics provide the lowest values of the amplitude functions $\beta^*_{x,y}$. Increasing the beam energy and thus, factor γ in Eq.(5), is, generally speaking of help too though, the task of the higher energy beam focusing requires stronger and more challenging magnets in the machine's interaction regions (IRs).

Figure 6: Peak luminosities of particle colliders (adapted from [3]).

Figure 6 demonstrates the impressive progress of luminosities of colliding beam facilities since the invention of the method. Again, the triangles are lepton colliders and full circles are for hadron colliders. One can see that over the last 50 years, the performance of the colliders has improved by more than 6 orders of magnitude and reached record high values of over 10^{34}cm^{-2}s^{-1}. At such luminosity, one can expect to produce, e.g., 100 events over one year of operation (about 10^7 s) if the reaction cross section is 1 femtobarn (fb)=10^{-39} cm^2. Table 2 summarizes the peak luminosity values and key beam parameters for proton-(anti)proton supercolliders.

Table 2: Luminosity and beam parameters of proton-proton/proton-antiproton superconducting supercolliders.

	$E_{\rm cm}$ TeV	Peak L, 10^{34} cm^{-2}s^{-1}	$N_{p(a)}$ 10^{11}	N_B	$\varepsilon_{p(a)}$ µm	β^* cm	ξ	W MJ
Tevatron	1.96	0.043	2.9/0.8	36	3/1.5	28	0.025	1.7
SSC	40	0.1	0.075	17,240	1	50	0.004	418
UNK	6	0.1	3	348	7.5	150	0.005	50
RHIC	0.5	0.025	1.9	111	3.1	65	0.018	0.8
LHC	14	1.0	1.15	2,808	3.7	55	0.01	360
FCC	100	5.0	1	10,600	2.2	110	0.01	8400

The total number of HEP reactions is of course, proportional to the luminosity integral $I=\int L dt$ and in the end, this is the most critical parameter for collider experiments. The integral depends on the total accelerator running time (typically – many years, decades for the supercolliders), the machine availability (ratio of the luminosity operation time to calendar time), and evolution of the luminosity in individual luminosity runs (sometimes also referred as “HEP stores”). Usually, the luminosity of a hadron collider decays with some characteristic time τ_L that may vary from a few hours to dozen(s) of hours depending on the machine - see Fig.7. Correspondingly, the integrated luminosity for the HEP stores longer than τ_L scales approximately as a product of the initial luminosity and the lifetime $I=\int L dt \approx L_0 \tau_L$.

Figure 7: One week luminosity record of the Tevatron proton-antiproton collider (May 1 - May 8, 2011), indicating individual HEP stores and characteristic luminosity decay in each store (see text).

Optimal performance of the supercolliders requires maximum integrated luminosity and minimizing the experimental background in the detectors (e.g., events created beams due to reasons different from the main collisions, such as scattering on the residual gas molecules, fast diffusion, etc.). Numerous issues which need to be addressed by accelerator designers and operators of the supercolliders are comprehensively presented and analyzed elsewhere – see, e.g., books [19, 20, 21] and reviews [5, 22] – and below we only briefly overview major integrated luminosity limitations in superconducting hadron colliders. They can be schematically divided in two categories – effects due to collisions (beam-beam effects, events pile-up, luminosity lifetime, etc.) and single-beam effects (single-particle stability and dynamic aperture (DA), impedance and collective effects, electron cloud effects, machine stability and noises leading to emittance growth, collimation and machine protection, particle production and cooling, space-charge effects, polarization, etc.).

2.1. *Beam-beam and other effects due to collisions*

In a hadron collider, the colliding beams must have small transverse dimensions to reach high luminosity – see Eq. (6). This leads to a strong electromagnetic force exerted by each beam on the particles of the other – see Fig.8. The beam-beam interactions usually result in strong enhancement of particle losses and emittance growth and reduction of the luminosity lifetime and luminosity integral (sometimes - in significant and fast beam intensity loss and quench of superconducting magnets). It is known to be one of the most severe limitations on the collider performance comprehensively studied and widely discussed by the accelerator physics community, see, e.g., proceedings of corresponding workshops and several review articles [23-29]. Table 2 shows that maximum *beam-beam parameter* ξ - the figure of merit of beam-beam interaction that equals the shift of the particles' betatron frequency (tune) due to the collisions – which could be operationally achieved in the hadron supercolliders colliders is:

$$\xi = N_{IP}\zeta_{IP} = N_{IP}\frac{N_p r_p}{4\pi\varepsilon} \leq 0.025 \; , \qquad (8)$$

where $r_p=e^2/mc^2=1.53\cdot10^{-18}$ m denotes the classical proton radius, N_p and ε are the opposite bunch intensity and emittance, correspondingly, and N_{IP} is the total number of head-on IPs.

Figure 7: Schematic dependence of the beam-beam force on proton vs the proton coordinate at the IP: it is de-focusing for proton-proton interaction (solid line) and focusing for interaction of proton with opposite change beam (antiprotons, electrons – see dashed line, scaled by factor of 2 for illustration purpose).

Contrary to *e-e+* colliders which usually enjoy fast synchrotron radiation damping of the betatron oscillations and where attempts to overcome the maximum beam-beam parameter of ξ*~0.05-0.1* lead to threshold-like performance degradation, the beam-beam limit in the hadron colliders is usually "soft" and indicates an approximate boundary between "optimal" and "barely operationally tolerable" conditions like particle losses, backgrounds, emittance growth and luminosity degradation rates, etc. Still, given that hadron machines are quite sensitive to much smaller tune changes $dQ_{x,y}$~0.001 off the optimal machine working point (Q_x, Q_y) it is remarkable how carefully these colliders' parameters are set to accommodate large tune spread of the order of ξ. For example, in the Tevatron collider, particles' vertical and horizontal tunes were between the 5th and 7th order resonances (between $Q_{x,y}$=3/5=0.6 and $Q_{x,y}$=4/7=0.571, the integer part of the tune [$Q_{x,y}$]=20) and the beam-beam tune spread fully covered the tune area – see Fig. 8.

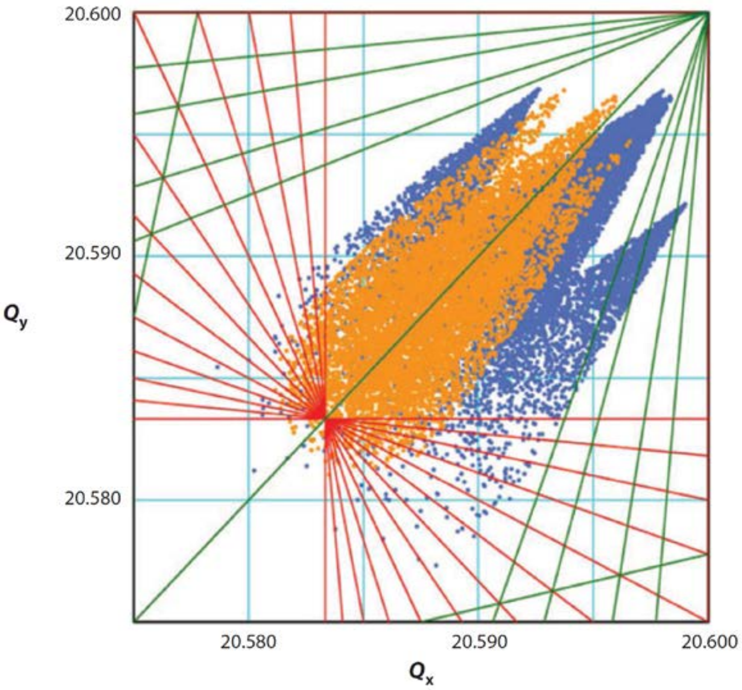

Figure 8 : Tevatron proton and antiproton tune distributions superimposed onto a resonance line plot. The red and green lines are various sum and difference tune resonances of up to the twelfth order. The blue dots represent the calculated tune distributions for all 36 antiproton bunches; the yellow represent the protons. The tune spread for each bunch is calculated for particles up to 6σ amplitude taking into account the *measured* intensities and emittances (from Ref.[30]).

An additional complication comes from operations with many bunches - dozens to thousands as indicated in Table 2 - which is driven by so called "events pile-up" phenomenon, characteristic for hadron colliders. Due to large cross sections of the total inelastic cross sections of proton-proton/proton-antiproton/proton-ion/ion-ion reactions, a significant number of beam particles disintegrate in each act of bunch-to-bunch collision, creating an entangled picture of events in the particle detectors which cannot be temporally resolved:

$$N_{pileup} = \frac{L\sigma_{inel}}{f_0 N_B} , \qquad (9)$$

where the inelastic events cross section is approximately σ_{inel} [mbarn]≈ 70+20 log *(E*[TeV]*)* [31]. To keep the number of events per bunch crossing sufficiently low under the condition of high average luminosity one needs to increase the number of bunches – indeed, in the Tevatron the pile-up was kept under N_{pileup}<15 with N_B=36 bunches, while the pileup of up to 30 is expected for the LHC at the design luminosity with N_B=2808 bunches.

Separation of two beams is needed to avoid multiple $2N_B$ collisions points which would immediately lead to unacceptable total beam-beam tuneshift parameters ξ – see Eq. (8) - and leave only one or a few dedicated IPs with head-on collisions. Such separation can be implemented either by the use of high-voltage (HV) electrostatic separators in single-aperture proton-antiproton colliders, like Tevatron, or by an independent aperture for each beam, like in RHIC (two magnetic systems) or in the LHC ("two-in-one" magnet with two beam openings, each having same but opposite magnetic fields). But even in the latter case, there are by necessity regions near the main IPs where to beams have to join each other in the same vacuum chamber. Usually these regions are much longer than the bunch-to-bunch spacing (longitudinal distance between neighboring bunches) and a significant number of such parasitic *long-range beam-beam* interactions between separated bunches can take place. For example, there 70 long-range encounters per revolution in the Tevatron and up to 120 in the LHC. Altogether they can produce significant, sometimes dominating effects on the beam dynamics. It is typical for hadron colliders that beams are brought to head-on collisions only at the very end of the preparatory part of the operational HEP store cycle. Therefore, the beam dynamics during preceding stages of injection, energy ramp, and the low-beta squeeze (focusing optics adjustment) is mostly driven by the long-range beam–beam effects. The parasitic interaction effects depend on the normalized radial separation S of the beams orbits [32,33,27], expressed in the units of the RMS betatron beam sizes $\sigma_{x,y\beta}$:

$$S = \sqrt{(\Delta x / \sigma_{x\beta})^2 + (\Delta y / \sigma_{y\beta})^2} \ . \qquad (10)$$

Experience in the Tevatron and the LHC is that even a few long-range encounters with S<5-6 could cause unsatisfactory losses. So, supercollider designers typically aim at the orbit separations of S~9 or so. The long-range interactions contribute a tune spread of about:

$$\Delta Q_{LR} \approx \sum_{parasitic\ encounters} \frac{2\xi_{IP}}{S^2} \ . \qquad (11)$$

The pattern of the long-range interactions and, hence, their strength differs for each bunch with especially large variations at the end of bunch trains. This makes all beam dynamics indicators dependent on the bunch position in the train of bunches. For example, in the Tevatron collider operating with three trains of 12 bunches in each beam that were observed: significant variations of the beam orbits of about 40 microns, of the betatron tunes - by as much ΔQ_{LR}≈0.005, of the coupling and of the chromaticities $\Delta Q'_{LR}= \Delta(dQ/(dp/p))_{LR}$ ≈6 [21]. It is not surprising that with such significant differences in the tunes and chromaticities, the antiproton and proton bunch intensity lifetime and emittance growth rates varied substantially from bunch to bunch (we will discuss that in more detail discussion in the following sections).

Other complications of the beam-beam interactions can come from the facts that bunch dimensions at the IPs are not always the same between two beams or between vertical and horizontal planes, or that beam intensities are sometimes significantly mismatched. Many other factors - like the presence of either external noises or machine impedance, synchrotron radiation damping or other means of beam cooling, nonlinear magnetic focusing components in the machine or collisions assisted by crab-cavities or crab-waist elements – can play a significant role, too. All in all, the beam-beam effects remain one of the most critical challenges for hadron supercolliders.

Let us use the Tevatron collider as an illustration of the importance of the beam-beam interactions. During the Collider Run II (2001-2011), the beam losses during injection, ramp and squeeze phases were mostly caused by beam-beam effects. Fig. 9 shows that early in Run II, combined beam losses only in the Tevatron (the last accelerator out of total 7 in the accelerator chain) claimed significantly more than half of the luminosity. Due to various improvements, losses have been reduced significantly down by some 20-30% in 2008-2009, paving the road to a many-fold increase of the luminosity. In “proton-only” or “antiproton-only” stores, i.e., without any collisions, the losses did not exceed 2-3% per specie. So, the remaining 8-10% proton loss and 2-3% antiproton loss even before the start of the HEP store was due to beam-beam effects and they correspondingly reduced the initial luminosity L_0.

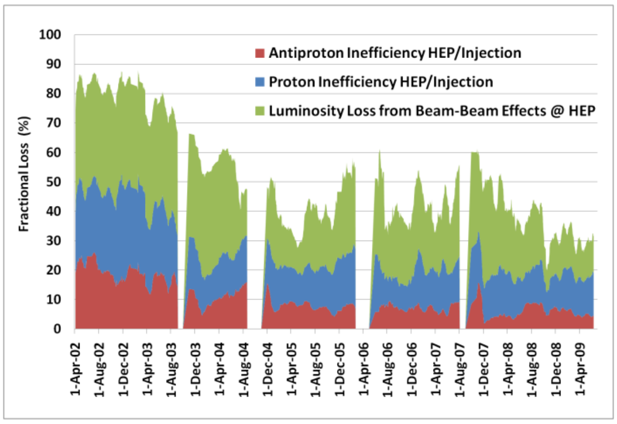

Figure 9: Evolution of the Tevatron beam losses in 2002-2009. Red shows fractional loss of antiprotons between injection into the Tevatron and start of collisions, next (blue) shows loss of protons, green – fractional reduction of the luminosity integral caused by beam-beam effects in collisions [34].

During the HEP stores, the Tevatron luminosity decay could be well approximated by a simple empirical fit with just two parameters - the initial luminosity L_0 and the initial luminosity lifetime τ_L [34]:

$$L(t) = \frac{L_0}{1 + t/\tau_L} , \qquad (12)$$

Correspondent luminosity integral for the store duration T depends on the product of the peak luminosity and the luminosity lifetime $I \approx L_0 \tau_L \ln(1 + T/\tau_L)$. From Eq.(6), the collider luminosity lifetime is determined by the speed of the emittance growth, proton and antiproton beam intensity loss rates, and bunch lengthening (that affects the geometric luminosity reduction factor *F*):

$$\tau_L^{-1} = \frac{dL(t)}{L(t)dt} = |\tau_\varepsilon^{-1}| + \tau_{Na}^{-1} + \tau_{Np}^{-1} + \tau_F^{-1}. \qquad (13)$$

At the end of Run II, the luminosity loss rates were in the range of 19-21 %/hr. at the beginning of stores, i.e., τ_L≈5 hours. For the 2010-2011 HEP stores in range of initial luminosities were between 3.0 and 4.3 10^{32} $cm^{-2}s^{-1}$, and the largest contribution to luminosity decay came from beam emittance growth with a typical time of τ_ε ~ 9-11 hrs. The growth was dominated by intrabeam scattering (IBS) in the proton bunches, with small contributions from the IBS in antiprotons and external noises. Beam-beam effects usually manifested themselves in the reduction of the beam emittances or their growth rates rather than in increases. The antiproton bunch intensity lifetime τ_a ~ 16-18 hours was dominated by the luminosity burn-up with a total cross section of about σ_{tot} [mbarn]≈ 70 mbarn – see Eq. (5) - which accounted for 80-85% of the lifetime, while the remaining 10-15% came from parasitic beam-beam interactions with protons. Proton intensity loss varied in a wide range τ_p ~ 25-45 hr. and was driven mostly (~50%) by the head-on beam-beam interactions with smaller size antiprotons at the main IPs. The proton lifetime caused by inelastic interactions with antiprotons in collisions and with residual gas molecules varies from 300 to 400 hours. The hourglass factor *F* decays with τ_F ~ 70-80 hours due to the IBS again, mostly in proton bunches. Beam-beam effects sometime lead to reduction of the proton bunch length growth (longitudinal “shaving”) in a poorly tuned machine. Combining all of these loss rates together, one can estimate the hit on the luminosity lifetime τ_L due to the beam-beam effects can be as much as 12-17% (that is equal to (2.5-3.5 %/hr.) out of total (19-21 %/hr.)). Therefore, the full impact of the beam-beam effects on the luminosity integral should include beam-beam driven proton and antiproton losses at the injection energy (about 5% and 1%, correspondingly), on the energy ramp (2% and 3%), and in the low-beta squeeze (1-2% and 0.5%) which proportionally reduce the initial luminosity L_0. So altogether, at the end of the Tevatron collider Run II operation, after about a decade of studies, improvements and optimizations, the beam-beam effects reduced the luminosity integral by 23-33% [21].

Operational implications of the beam-beam interactions in RHIC and LHC are similarly serious [34, 35].

2.2. *Single beam issues in hadron colliders*

Besides the issues related to beam-beam interactions, many challenges arise from one-beam phenomena specific for hadron supercolliders and driven by the quest for higher luminosity. Comprehensive analysis of them is beyond the scope of this book so we only provide a brief overview of them. An interested reader can be referred to detailed reviews in, e.g., [12, 21, 37, 38]. Taking into account the beam-beam tuneshift limit (8), the luminosity equation (6) can be re-written as:

$$L = \xi \cdot \frac{I}{e} \cdot \frac{\gamma}{\beta^*} \cdot \frac{F}{r_p} \quad , \qquad (14)$$

where $I=efN_BN_p$ is the single beam total current, $\gamma=E/mc^2$ is relativistic factor and e is the proton charge. The form factor F is always tried to be set as close to 1 as possible, so the focus of the luminosity maximization efforts under the condition of the beam-beam limit on parameter ξ usually goes towards an increase of the total beam current I and reduction of the beta-function β^* at the IPs.

The issues associated with high-current operation are numerous and start with the beam production. One of the most severe limitations is set by space-charge forces in the low-energy accelerators in the collider injection chain which lead to unacceptable emittance growth and particle losses if the space-charge tuneshift parameter:

$$-\Delta Q_{SC} = \frac{N_p r_p B_f}{4\pi\varepsilon_n \beta_p \gamma^2} \quad , \qquad (15)$$

exceeds a certain value, typically about ~0.3 (here $\beta_p=v_p/c$ and γ are relativistic parameters, B_f is the bunching factor – ration of peak current to average current) [39,40]. Production and accumulation of secondary particles, such as antiprotons has its own set of challenges associated with the need of the beam cooling [41, 21]. High current proton beams are subject of various collective instabilities both in the injectors and collider rings caused by machine impedance [42] and electron-cloud initiated by either particle losses or by synchrotron radiation [43]. Various cures are being implemented to keep such high intensity beams stable, including minimization of the impedance, feedback systems to damp beam oscillations, introduction of non-linear focusing elements to induce stabilizing tune spread in the beams, operation at higher chromaticities $Q'=dQ/(dp/p)$, special coating or beam scrubbing of the beam vacuum chambers by enhanced proton losses to suppress formation of the electron cloud, etc.

One of the biggest challenges for energy frontier superconducting colliders is safe absorption of ever growing energy $W=IE/f$ carried by the beams – see Table 2 - and beam backgrounds. For example, in the LHC, with I=0.5 A of circulating current and at E=7 TeV beam energy, the stored energy is W=360 MJ per beam in the nominal conditions – see Fig.10 a). Even the modest loss rates of 1 % of the stored intensity in a period of about 10s would produce a peak power load of 500kW. That surely would pose a high risk as the quench limit in the main LHC magnet is about 8 W/m. Sophisticated collimation systems are required to protect the machine and the HEP detectors from beam losses and particle halo backgrounds. A two-stage collimation system of the Tevatron collider comprised of 14 collimators successfully handled some 2MJ of beam energy at 1 TeV [45], while 108 collimators were installed in the LHC three-stage collimation system to guarantee inefficiencies of less or about $2\cdot10^{-5}$ per m of accelerator for a circulating current of $3\cdot10^{14}$ protons per beam [46] – see Fig.10. To assure minimal inefficiency - defined as unwanted fractional leakage of high energy particles from the collimation system onto critical machine elements, such as SC magnets - the collimators need to be placed within fractions of a mm to the beam and become very troublesome dominating sources of impedance which in turn can limit the maximum machine current [47]. Due to smaller beam size and higher beam energy, record high energy densities in the LHC and future hadron supercolliders – shown in Fig.10 b) - pose serious concerns about the collimator material robustness against regular beam losses and accident scenarios [46].

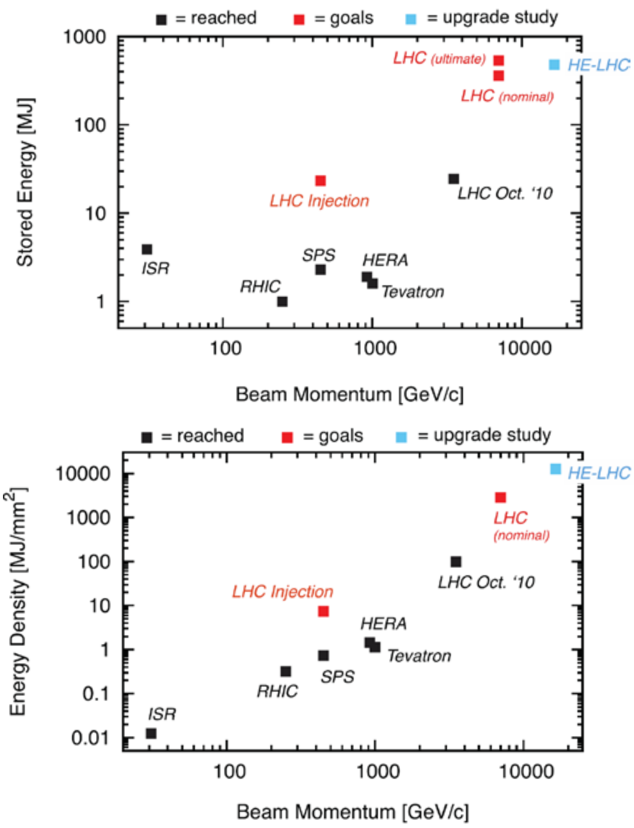

Figure 10: (a- left) Stored energy per beam versus beam momentum for record high intensity and energy accelerators. The black squares indicate achieved values, red squares show design values and the blue square represents the HE-LHC design [38]. (b- right) Energy density versus beam momentum (from [44]).

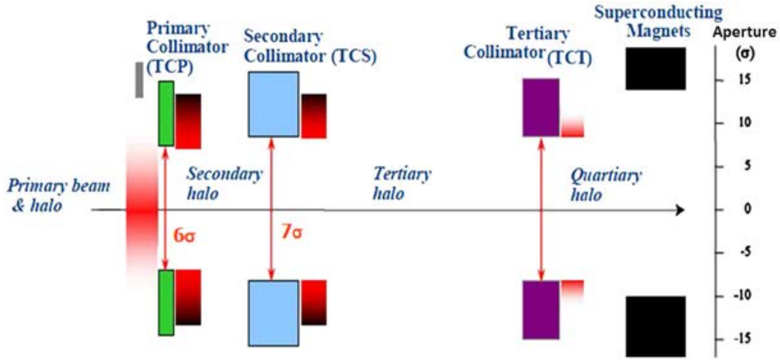

Figure 11: Schematic diagram of the LHC three-stage collimation system: the primary collimator jaws are positioned closest to the beam while the jaws of the secondary and tertiary collimators are retracted further away from the beam (from [46]).

Stringent requirements on beam loss in supercolliders, puts additional emphasis on orbit control and ground motion drifts [48], intrabeam and gas scattering, external noises [21], single particle diffusion due to nonlinear resonances, etc.

3. Discussion: Accelerator R&D Towards a 100 TeV *p-p* Collider

An extensive, decadal accelerator R&D program is needed to prove the feasibility of a 100 TeV circular proton-proton collider. The program has to demonstrate significant progress compared to the current state-of-the-art in three areas: a) “feasibility of energy” – development of the 16-20 T SC magnets of accelerator quality; b) “feasibility of performance” – resolution of the beam issues relevant to attainment of the design luminosity; and c) “feasibility of cost” – practical solutions of numerous issues related to financing of the construction and support of operation of a 100 km long accelerator. The planning work on the development of the record high field accelerator magnets has started [49]. The proposed program has four major objectives:

1. Develop accelerator magnets at the limit of Nb_3Sn capabilities (16-20 T);
2. Investigate accelerator magnet designs with Low Temperature Superconductor (LTS) and High Temperature Superconductor (HTS) coils for fields beyond the capability of Nb_3Sn;
3. Drive high-field conductor development, including Nb_3Sn and HTS materials for high-field accelerator magnets;
4. Address fundamental aspects of magnet design, technology and performance that could lead to substantial reductions of magnet cost.

The program relies upon a collaborative effort of larger international community of magnet designers in the US, Europe and Asia, industry and universities that takes maximum advantage of existing infrastructure and expertize at the participating institutions.

The ultimate goal of an integrated luminosity for a 100 TeV p-p collider is thought to be in the range of 10-20 ab^{-1} per experiment, corresponding to an ultimate instantaneous luminosity approaching 2×10^{35} $cm^{-2}s^{-1}$ [50]. It is not clear yet whether that goal can be achieved because of the issues due to the beam-beam interactions, electron cloud and space charge effects, particle losses and collimation, absorption of MW's of the synchrotron radiation power in the superconducting magnet environment, coherent beam stability at injection energy, challenging requirements on the proton injection complex, beam RF acceleration systems, etc. Corresponding R&D programs has been launched in Europe and in China [13, 51, 52]. One can imagine that many if not all of the current advanced methods will need to be employed at the energy frontier collider, including beam-beam compensation [53-57], space-charge compensation [58-61], novel collimation using hollow electron beams or bent crystals [62-64, 45, 65], photon stops [66, 67], non-linear integrable optics [68, 69], etc. It might be of great help for the accelerator builders to be allowed to design the machine with less aggressive luminosity goals, e.g., $O(10^{33}$ $cm^{-2}s^{-1}$), and count on continuous luminosity improvements which we often have seen in colliders [70]. As noted in Ref.[50]: "…For a large class of new-physics scenarios that may arise from the LHC, less aggressive luminosity goals are acceptable as a compromise between physics return and technical or experimental challenges. In particular, even luminosities in the range of 10^{32} $cm^{-2}s^{-1}$ are enough to greatly extend the discovery reach of the 100 TeV collider over that of the HL-LHC, or to enhance the precision in the measurement of discoveries made at the HL-LHC."

Finally, the cost of the facility is expected to be high and one of the biggest challenges is to find ways to make it not as prohibitively high as predicted by the phenomenological $\alpha\beta\gamma$-cost model [15] – see Eq.(4). While SC magnets usually dominate the construction cost of the supercolliders and factor of ~(2-3) cost reduction (per TeV) of the magnet technology is needed compared to the LHC, other cost drivers – such as civil construction and power infrastructure – should be heavily cost optimized as well. Opportunities to re-use existing accelerator tunnels, laboratory infrastructure and electric grid power capabilities might become critical. Obviously, regional differences in the accounting practices for construction of larger scientific facilities in the US, Europe and Asia can also play significant role in the overall feasibility analysis of the next generation energy frontier hadron supercolliders.

Acknowledgments

This note was presented and discussed at the "Workshop on the future of high energy physics" held at the Jockey Club Institute for Advanced Study of the Hong Kong University of Science and Technology, January 5-30, 2015. I would like thank Henry Tye and the staff of the Institute for the hospitality, and Prudence Wong for helpful practical assistance. In particular, I acknowledge stimulating discussions with Chris Quigg, Charlie

Young, Ian Hinchliffe, Michelangelo Mangano, Stephen Gourlay, Dick Talman, Yunhai Cai, Qin Qing and Yifang Wang.

References

1. E.Haussecker, A.Chao, *Physics in Perspective* **13,** 146 (2011).
2. M.Tigner, A.Chao (Eds.), *Handbook of Accelerator Physics and Engineering* (World Scientific, Singapore, 1999)
3. V.Shiltsev, *Physics-Uspekhi* **55.10,** 965 (2012)
4. M.Tigner, *Nuovo Cimento* **37,** 1228 (1965)
5. S.Holmes, V.Shiltsev, *Annu. Rev. Nucl. Part. Sci.* **63**, 435-465 (2013)
6. L.Evans, *Annu. Rev. Nucl. Part. Sci.* **61**, 435-466 (2011)
7. A.Tollestrup, E.Todesco, *Rev. Accel. Sci. Tech.* **1,** 185-210 (2008)
8. M. Harrison, S.Peggs, T.Roser, *Annu. Rev. Nucl. Part. Sci.* **52.1**, 425-469 (2002).
9. *SSC Conceptual Design,* SSC-SR-2020, SSC Laboratory (1986)
10. V.Yarba, in *Proceedings of IEEE PAC'91* (San Francisco, CA, 1991), p. 2913
11. S. Wojcicki, *Rev. Accel. Sci. Tech.* **2**, 265 (2009)
12. VLHC Design Study Group, *Design study for a staged very large hadron collider*, FERMILAB-TM-2149 (2001)
13. F.Zimmermann, et al., in *Proceedings of IPAC2014* (Dresden, Germany, 2014), p. 1
14. O.Bruning, P.Collier, *Nature* **448**, 285-289 (2007)
15. V.Shiltsev, *JINST* **9** T07002 (2014)
16. L.Teng, FERMILAB-FN-461 (1987)
17. V.Yarba, private communication (2014)
18. L.Rossi, L.Bottura, *Rev. Accel. Sci. Tech.* **5,** 51-89 (2012)
19. Y.Yan, J.Naples, M.Syphers (eds.), *Accelerator Physics at the Superconducting Super Collider* (AIP Conference Proceeding 326, AIP, New York, 1995)
20. S.Myers, H.Schopper (eds.), *Elementary Particles-Accelerators and Colliders,* Landolt-Bornstein: Numerical Data and Functional Relationships in Science and Technology-New Series/Elementary Particles, Nuclei and Atoms, **21** (Springer-Verlag, Berlin, 2013)
21. V.Lebedev, V.Shiltsev (eds.), *Accelerator Physics at the Tevatron Collider* (Springer, New York, 2014)
22. W.Scandale, *Rev. Accel. Sci. Tech.* **7**, 9 (2014)
23. I.A. Koop , G.M. Tumaikin (Eds.), Proc. *3rd Advanced ICFA Beam Dynamics Workshop on Beam-Beam Effcets in Circular Colliders* (Novosibirsk, USSR, May 29 - June 3, *1989*).
24. J.Poole and F. Zimmermann (eds.), Proc. Workshop on Beam-Beam Effects in Large Hadron Colliders (Geneva, April 12-17, 1999), CERN-SL-99-039 AP (1999)
25. J.Wei, W.Fischer. P.Manning (eds.), Proc. *29th ICFA Beam Dynamics Workshop HALO'03* and *Workshop on Beam-Beam Interactions BEAM-BEAM'03* (AIP Conference Proceeding 693, AIP, New York, 2003)
26. W.Herr, G.Papotti (eds.), Proc. *ICFA Mini-Workshop on Beam-Beam Effects in Hadron Colliders* (18 - 22 March, 2013, CERN, Geneva, Switzerland), CERN-2014-004 (2014)
27. T. Sen, et al, *Phys. Rev. ST Accel. Beams* **7**, 041001 (2004)
28. V. Shiltsev, et al., *Phys. Rev. ST Accel. Beams* **8**, 101001 (2005)
29. W.Fischer (Ed.), *ICFA Beam Dynamics Newsletter* **52** (2010)
30. V. Shitsev *et al*., *New Journal of Physics,* **10** 043042 (2008)
31. K.Olive, et al. (Particle Data Group), *The Review of Particle Physics*, Chin. Phys. C **38**, 090001 (2014).
32. D. Siergiej, D. Finley, W. Herr, *Phys. Rev. E* **55**, 3521 (1997)

33. Y.Papaphilippou, F.Zimmermann, *Phys. Rev. ST Accel. Beams* **5**, 074001 (2002)
34. R.Moore, A.Jansson, V.Shiltsev, *JINST* **4** P12018 (2009)
35. see, e.g., Y.Luo and W.Fischer, in Reference [26], pp.19-25.
36. see, e.g., G.Papotti, et al, in Reference [26], pp.1-5.
37. O. Brüning, et al., *The LHC Design Report*, CERN Technical Report (CERN, Geneva, 2004) http://ab-div.web.cern.ch/ab-div/Publications/LHC-designreport.html
38. E.Todesco, F.Zimmermann (Eds.), Proc. *EuCARD-AccNet-EuroLumi Workshop "The High Energy Large Hadron Collider"* (14-16 October, 2010, Malta), CERN-2011-003 (2011).
39. A.Luccio, W.Weng (Eds.), Proc. *Workshop on Space Charge Physics in High Intensity Hadron Rings* (May 4-7, 1998, Shelter Island, NY), *AIP Conference Proceedings* **448** (AIP, New York, 1998)
40. See, e.g., presentations at the "SPACE CHARGE 2013" Workshop (16-19 April 2013, CERN) at: https://indico.cern.ch/event/221441/
41. M.Church, J.Marriner, *Annu. Rev. Nucl. Part. Sci.* **43**, 253-295 (1993).
42. K.Y. Ng, *Physics of intensity dependent beam instabilities* (World Scientific, Singapore, 2006)
43. R.Cimino, G.Rumolo, F.Zimmermann (eds.), Proc. *ECLOUD'12: Joint INFN-CERN-EuCARD-AccNet Workshop on Electron-Cloud Effects* (5-9 Jun 2012, La Biodola, Italy), Preprint CERN-2013-002 (2013)
44. see R.Assmann in Ref.[38], pp.124-127.
45. N.Mokhov, et al, *JINST* **6** T08005 (2011)
46. M.Cauchi, et al, *Phys. Rev. ST Accel. Beams* **17**, 021004 (2014)
47. H.Burkhardt et al, in *Proceedings of IEEE PAC'05* (Knoxville, TN, 2005), p.1132
48. V.Shiltsev, *Phys. Rev. ST Accel. Beams* **13**, 094801 (2010)
49. G.Apollinari, et al, Fermilab Preprint FN-0993-TD (2015).
50. I.Hinchliffe, et al, arxiv:1504.06108
51. M.Benedikt, CERN preprint FCC-PUB-PP-0014 (2014)
52. Y.Wang, in *Proceedings of IPAC2015* (Richmond, VA, USA, 2015), FRIGB2
53. V.Shiltsev, V.Danilov, D.Finley, A.Sery, *Phys. Rev. ST Accel. Beams* **2(7)**, 071001 (1999).
54. V.Shiltsev *et al*., *Phys. Rev. ST Accel. Beams* **11**, 103501 (2008)
55. V.Shiltsev, *et al*., *Phys.Rev.Lett.* **99**, 244801 (2007)
56. V.Shitsev, *et al*., *New Journal of Physics*, **10**, 043042 (2008)
57. Y.Luo, *et al, Phys. Rev. ST Accel. Beams* **15**, 051004 (2012)
58. A.Burov, G.Foster, V.Shiltsev, FNAL-TM-2125 (2000)
59. Y.Alexahin, et al., in *Proceedings IEEE PAC'2007* (Albuquerque, NM, USA, 2007), p.3474
60. V.Shiltsev, et al, *AIP Conf. Proceedings* **1086**, 649 (2009)
61. V.Litvinenko, G.Wang. *Phys. Rev. ST Accel. Beams* **17** (11), 114401 (2014)
62. V.Shiltsev, in *Proceedings of the 3rd CARE-HHH-APD Workshop* (LHC-LUMI-06, Valencia, Spain), p. 92; CERN-2007-002 (2007)
63. G.Stancari et al., *Phys. Rev. Lett.* **107**, 084802 (2011)
64. S.Radaelli, et al., in *Proceedings of IPAC2015* (Richmond, VA, USA, 2015), WEBB1
65. V.M.Biryukov, et al. *Nuclear Instruments and Methods in Physics Research Section B: Beam Interactions with Materials and Atoms* **234.1,** 23 (2005)
66. P.Bauer, et al. *Proceedings of the 2001 IEEE Particle Accelerator Conference* (Chicago, IL, USA, 2001), p.3156
67. W.Barletta, et al., *Nuclear Instruments and Methods in Physics Research Section A: Accelerators, Spectrometers, Detectors and Associated Equipment* **764,** 352 (2014)
68. V.Danilov, V.Shiltsev, Preprint FERMILAB-FN-0671 (1998)
69. V.Danilov, S.Nagaitsev, Phys. Rev. ST Accel. Beams **13**, 084002 (2010).
70. V. Shiltsev, *Mod. Phys. Lett.* **A 26,** 761 (2011)